

# Robust Subspace Clustering With Compressed Data

Guangcan Liu<sup>1</sup>, Senior Member, IEEE, Zhao Zhang<sup>2</sup>, Senior Member, IEEE,  
Qingshan Liu<sup>3</sup>, Senior Member, IEEE, and  
Hongkai Xiong<sup>4</sup>, Senior Member, IEEE

**Abstract**—Dimension reduction is widely regarded as an effective way for decreasing the computation, storage, and communication loads of data-driven intelligent systems, leading to a growing demand for statistical methods that allow analysis (e.g., clustering) of compressed data. We therefore study in this paper a novel problem called *compressive robust subspace clustering*, which is to perform robust subspace clustering with the compressed data, and which is generated by projecting the original high-dimensional data onto a lower-dimensional subspace chosen at random. Given only the compressed data and sensing matrix, the proposed method, *row space pursuit (RSP)*, recovers the authentic row space that gives correct clustering results under certain conditions. Extensive experiments show that RSP is distinctly better than the competing methods, in terms of both clustering accuracy and computational efficiency.

**Index Terms**—Subspace clustering, compressive sensing, sparsity, low-rankness.

## I. INTRODUCTION

ALONG with the evolvement of data collection technology, the dimension of data is now getting higher and higher. For example, one can easily use the latest camera phones to take high-quality photos in a resolution of 40 or more megapixels. In general, when the data dimension increases, the cost in storing, transmitting and analyzing data will inevitably rise. What is more, the increase in data dimension is actually much faster than the advance in communication, storage and computation power. As a consequence, it is often desirable to reduce the dimensionality of data. However, given that the data of interest has been compressed via dimension reduction, a natural question to ask is *how to*

*analyze the structure of the original data by only accessing the compressed data.*

To investigate the highlighted problem, one essentially needs to integrate dimension reduction and pattern analysis into a unified framework. Among various dimension reduction methods, we would like to consider the well-known Random Projection (RP) [1], in which the original  $m$ -dimensional data points are projected to a  $p$ -dimensional ( $p \ll m$ ) subspace, using some sensing matrix  $R \in \mathbb{R}^{p \times m}$  generated at random. Unlike the data-dependent methods such as Principal Component Analysis (PCA) and Principal Component Pursuit (PCP) [2], which must be trained before being applied to the data, RP needs no training procedure and is therefore computationally efficient. Even more, the sensing matrix  $R$  is randomly generated and thus could be shared across multiple devices without transmission. Due to these advantages, RP is often the most preferable choice for reducing the dimension of data stored on resource-constrained devices, e.g., satellite-borne sensors [3]. Regarding the pattern analysis problems, *robust subspace clustering* [4]–[7], the task of grouping together the data points lying approximately on the same (linear) subspace, has considerable practical and scientific significance. In fact, as pointed out by [8], robust subspace clustering is a representative setting of unsupervised learning. So, in the spirit of unifying data compression with pattern analysis, we would suggest considering the following problem that combines RP with robust subspace clustering.

*Problem 1 (Compressive Robust Subspace Clustering):*

Let  $X = [x_1, \dots, x_n] \in \mathbb{R}^{m \times n}$  store a collection of  $n$   $m$ -dimensional points approximately drawn from a union of  $k$  subspaces. Suppose that  $R \in \mathbb{R}^{p \times m}$  ( $p \ll m$ ) is a random Gaussian matrix whose columns have unit lengths. Denote  $M \triangleq RX \in \mathbb{R}^{p \times n}$ . Given the compressed data  $M$  and the sensing matrix  $R$ , the goal is to segment all points into their respective subspaces.

Due to its significance in science and application, robust subspace clustering has received extensive attention in the literature, e.g., [5]–[7], [9]–[30]. However, most existing methods are specific to the original uncompressed data  $X$ , and we have spotted only sparse researches relevant to the setup of Problem 1. Namely, in [31], [32], it is shown that the subspace principal angles before and after RP compression are mostly unchanged, which means that one may simply input  $M$  into some existing subspace clustering methods such as Shape Interaction Matrix (SIM) [13], Sparse Subspace Clustering (SSC) [16], [33] and Low-Rank

Manuscript received January 1, 2019; revised April 23, 2019; accepted May 15, 2019. Date of publication May 24, 2019; date of current version August 14, 2019. This work was supported in part by the National Natural Science Foundation of China (NSFC) under Grant 61622305, Grant 61825601, Grant 61532009, Grant 61672365, Grant 61425011, Grant 61720106001, and Grant 61529101, in part by the Natural Science Foundation of Jiangsu Province of China (NSFJPC) under Grant BK20160040, and in part by the SenseTime Research Fund. The associate editor coordinating the review of this manuscript and approving it for publication was Dr. Emanuele Salerno. (Corresponding author: Guangcan Liu.)

G. Liu is with B-DAT and CICAET, School of Automation, Nanjing University of Information Science and Technology, Nanjing 210044, China (e-mail: gcliu@nuist.edu.cn).

Z. Zhang is with the School of Computer Science and Technology, Soochow University, Suzhou 215006, China (e-mail: cszzhang@gmail.com).

Q. Liu is with B-DAT, School of Automation, Nanjing University of Information Science and Technology, Nanjing 210044, China (e-mail: qslu@nuist.edu.cn).

H. Xiong is with the Department of Electronic Engineering, Shanghai Jiao Tong University, Shanghai 200240, China (e-mail: xionghongkai@sjtu.edu.cn).

Digital Object Identifier 10.1109/TIP.2019.2917857

Representation (LRR) [6], [25]. This, however, may not work for Problem 1, in which the original data  $X$  could be contaminated by gross errors; namely,

$$X = L_0 + S_0,$$

where  $L_0$  stores the authentic samples lying exactly on the subspaces and  $S_0$  corresponds to the possible errors. In the presence of gross errors, i.e., the entries in  $S_0$  have large magnitudes, it will lead to very poor results by simply applying subspace clustering methods to the compressed data  $M$ . This is because the projection procedure could change the statistical properties of the errors. For example, consider the case where the gross errors are entry-wisely sparse; that is, a small fraction of the entries in  $S_0$  are nonzero and have large magnitudes. In the compressed data matrix  $M$ , however, the errors may spread to every entries of the matrix, thereby  $RS_0$  is often a dense matrix with large values. The resulted problem—segmenting the points in  $M$  into correct subspaces purely based on  $M$  which itself is corrupted by dense gross errors—is indeed intractable.

In order to study Problem 1 under the context of sparse errors, we propose a simple yet effective method termed *row space pursuit* (RSP). Given the compressed data matrix  $M$  and sensing matrix  $R$ , RSP recovers not only the row space of the clean data (i.e.,  $L_0$ ) but also the possible gross errors. Since the authentic row space (i.e., row space of  $L_0$ ) provably determines the true subspace membership of the data points, the final clustering results are obtained by simply using the recovered row space as input to perform K-Means clustering. In general, RSP owns a computational complexity of only  $O(mnp)$  and can therefore fast segment a large number of high-dimensional data points. What is more, most of the computational resources required by RSP are spent on matrix multiplications, which are easy to accelerate by parallel algorithms. Extensive experiments on high-dimensional and large-scale datasets demonstrate the superior performance of RSP, in terms of both clustering accuracy and computational efficiency. In effect, RSP can even maintain comparable accuracies to the prevalent methods that perform clustering using the original high-dimensional, uncompressed data.

## II. PROBLEM FORMULATION AND ANALYSIS

Formally, the regime underlying a collection of points approximately drawn from a union of  $k$  subspaces could be modeled as  $X = L_0 + S_0$ , where  $L_0$  and  $S_0$  correspond to the components of the authentic samples and possible errors, respectively. The word “error”, in general, refers to the deviation between the model assumption (i.e., subspaces) and the observed data. In practice, the errors could exhibit as white noise [34], missing entries [35], outliers [25], [36] and corruptions [2]. In this paper, we would like to focus on the setting of gross corruptions studied in PCP [2]; namely,  $S_0$  is entry-wisely sparse and the values in  $S_0$  are arbitrarily large.

As shown in [6], [13], and [18], the row space of  $L_0$  can lead to exact subspace clustering under certain conditions. Hence, Problem 1 would be mathematically formulated as a problem called *compressive row space recovery*:

*Problem 2 (Compressive Row Space Recovery):* Let  $L_0 \in \mathbb{R}^{m \times n}$  with (skinny) SVD  $U_0 \Sigma_0 V_0^T$  and rank  $r_0$  store a set of  $n$   $m$ -dimensional authentic samples strictly drawn from a union of  $k$  subspaces, where  $V_0 \in \mathbb{R}^{n \times r_0}$ . Let  $R \in \mathbb{R}^{p \times m}$  ( $r_0 < p \ll m$ ) be a random Gaussian matrix whose columns have unit  $\ell_2$  norms. Suppose that the data matrix  $X$  is generated by  $X = L_0 + S_0$ , with  $S_0$  being an entry-wisely sparse matrix corresponding to the possible errors. Denote by  $M \triangleq RX \in \mathbb{R}^{p \times n}$  the compressed data matrix. Given  $M$  and  $R$ , the goal is to identify  $V_0 V_0^T$  and  $S_0$ .

The above problem is essentially a generalization of the *subspace recovery* problem studied in [6]. To approach Problem 2, one may consider Compressive Sparse Matrix Recovery (CSMR) [37], which is a variation of Compressive Principal Component Pursuit (CPCP) [38]. Given  $M$  and  $R$ , CSMR strives to recover  $RL_0$  and  $S_0$  by solving the following convex optimization problem:

$$\min_{A \in \mathbb{R}^{p \times n}, S \in \mathbb{R}^{m \times n}} \|A\|_* + \lambda \|S\|_1, \quad \text{s.t. } M = A + RS, \quad (1)$$

where  $\|\cdot\|_1$  denotes the  $\ell_1$  norm of a matrix seen as a long vector. Under certain conditions, it is provable that CSMR strictly succeeds in recovering both  $RL_0$  and  $S_0$ . However, as clarified in [37], CSMR is actually designed for the case where  $m \gg n \gg r_0$ , i.e.,  $L_0$  is a tall, low-rank matrix such that  $RL_0$  is still low rank. In the cases of square or fat matrices, the recovery ability of CSMR is quite limited, because in this case  $RL_0$  could be high rank or even full rank. To achieve better results, we shall propose a new method termed RSP.

## III. COMPRESSIVE ROBUST SUBSPACE CLUSTERING VIA ROW SPACE PURSUIT

In this section, we shall detail the proposed RSP method for compressive robust subspace clustering.

### A. Compressive Row Space Recovery by RSP

The formula of RSP is derived as follows. Denote by  $U_0 \Sigma_0 V_0^T$  and  $r_0$  the SVD and rank of  $L_0$ , respectively. Since  $M = R(L_0 + S_0)$ , we could construct a matrix  $P \in \mathbb{R}^{n \times n}$  to annihilate  $L_0$  on the right, i.e.,  $L_0 P = 0$ . This can be easily done by taking  $P = \mathbb{I} - V_0 V_0^T$ , with  $\mathbb{I}$  being the identify matrix. That is,

$$(M - RS_0)(\mathbb{I} - V_0 V_0^T) = RL_0(\mathbb{I} - V_0 V_0^T) = 0. \quad (2)$$

Hence, we may seek both  $V_0$  and  $S_0$  by the following non-convex program:

$$\min_{V \in \mathbb{R}^{n \times r}, S \in \mathbb{R}^{m \times n}} \|S\|_1, \\ \text{s.t. } (M - RS)(\mathbb{I} - VV^T) = 0, \quad V^T V = \mathbb{I}, \quad (3)$$

where  $r$  ( $r_0 \leq r < p$ ) is taken as a parameter. In order to attain an exact recovery to the authentic row space  $V_0$ , we would need  $r = r_0$ . Yet, to obtain superior clustering results in practice, exact recovery is not indispensable, and it is indeed unnecessary for the parameter  $r$  to strictly equal to the true rank  $r_0$ , as will be shown in our experiments. There is also an intuitive explanation for this phenomenon. That is,

the equality in (2) always holds when  $V_0$  is replaced by any other space that includes  $V_0$  as a subspace.

**Analysis:** We shall briefly analyze the performance of the RSP program (3), under the context of Problem 2. To do this, we first consider an equivalent version of (3):

$$\min_{P,S} \|S\|_1, \quad \text{s.t. } (M - RS)(\mathbb{I} - P) = 0, \quad P \in \Xi, \quad (4)$$

where  $\Xi = \{VV^T : V \in \mathbb{R}^{n \times r}, V^T V = \mathbb{I}\}$  is the set of orthogonal projections onto a  $r$ -dimensional subspace. For the sake of simplicity, assume that  $r = r_0$ . Whenever  $S = S_0$ , it is provable that  $P = V_0 V_0^T$  is the only feasible solution to the problem in (4). More precisely, provided that  $p \geq r_0$ , it is almost surely (i.e., with probability 1) that the row space of  $RL_0$  is exactly  $V_0$  [39]. On the other hand, given  $P = V_0 V_0^T$ , the problem in (4) turns into a *sparse signal recovery* problem explored in [40]; namely,

$$\min_y \|y\|_1, \quad \text{s.t. } b = \Phi y, \quad (5)$$

where  $\Phi = (\mathbb{I} - V_0 V_0^T) \otimes R$  and  $b = \text{vec}(M(\mathbb{I} - V_0 V_0^T))$ . Here, the symbols  $\otimes$  and  $\text{vec}(\cdot)$  denote the Kronecker product and the vectorization of a matrix into a long vector, respectively. Since  $\mathbb{I} - V_0 V_0^T$  is an orthogonal projection,  $\Phi$  may still satisfy the so-called Restricted Isometry Property (RIP) [40]. As a result, according to [40], the convex program in (5) may identify  $\text{vec}(S_0)$  with overwhelming probability, as long as  $p \geq c \|S_0\|_0/n$  for some numerical constant  $c$ , where  $\|\cdot\|_0$  is the  $\ell_0$  pseudo-norm of a matrix, i.e., the number of nonzero entries of a matrix.

In summary, the results in [39] and [40] have already proven that  $(P = V_0 V_0^T, S = S_0)$  is a critical point to the non-convex problem in (4). However, due to the orthonormal constraint  $V^T V = \mathbb{I}$ , it would be hard to obtain a stronger guarantee. Thus, in this paper we would like to focus on the empirical performance of RSP. Still, the above analysis provides some useful clues for understanding the behaviors of RSP. Namely, to obtain exact or near exact recoveries to  $V_0 V_0^T$  and  $S_0$ , the number of random projections  $p$  has to obey the following two conditions:

$$p \geq r_0 \quad \text{and} \quad p \geq c \|S_0\|_0/n. \quad (6)$$

For convenience, hereafter, we shall consistently refer to the quantity  $\|S_0\|_0/n$  as the *corruption size*.

### B. Optimization Algorithm

The observed data in reality is often contaminated by noise, and thus we shall consider instead the following non-convex program that can also approximately solve the problem in (3):

$$\min_{V \in \mathbb{R}^{n \times r}, S \in \mathbb{R}^{m \times n}} \lambda \|S\|_1 + \frac{1}{2} \|(M - RS)(\mathbb{I} - VV^T)\|_F^2, \quad \text{s.t. } V^T V = \mathbb{I}, \quad (7)$$

where  $\|\cdot\|_F$  denotes the Frobenius norm of a matrix and  $\lambda > 0$  is a parameter.

Although non-convex as a whole, the problem in (7) is indeed easy to solve while one of  $V$  and  $S$  is given, thereby it is suitable to solve (7) by the first-order methods established

---

### Algorithm 1 Solving the Problem in (7) by the Alternating Proximal Method

---

- 1: **input:**  $M, R, r$  and  $\lambda$ .
  - 2: **parameters:**  $\rho = 1.1 \|R\|^2$
  - 3: **Output:**  $V$  and  $S$ .
  - 4: **Initialization:**  $S = 0$ .
  - 5: **repeat**
  - 6:   compute the matrix  $M - RS$ .
  - 7:   update  $V$  using the top  $r$  right singular vectors of  $M - RS$ .
  - 8:   compute the gradient given in (9).
  - 9:   update  $S$  by (10).
  - 10: **until** convergence
- 

in the literature [41]–[43]. We choose to use the alternating proximal method established in [43]. Let  $(V_t, S_t)$  be the solution estimated at the  $t$ th iteration. Denote

$$g(V, S) \triangleq \frac{1}{2} \|(M - RS)(\mathbb{I} - VV^T)\|_F^2.$$

Then the solution to (7) is updated via iterating the following two procedures:

$$\begin{aligned} V_{t+1} &= \arg \min_V g(V, S_t), \quad \text{s.t. } V^T V = \mathbb{I}, \\ S_{t+1} &= \arg \min_S \frac{\lambda}{\rho} \|S\|_1 + \frac{1}{2} \|S - (S_t - \frac{\partial_S g(V_{t+1}, S)}{\rho})\|_F^2, \end{aligned} \quad (8)$$

where  $\rho > 0$  is a penalty parameter and  $\partial_S g(V_{t+1}, S)$  is the partial derivative of  $g(V, S)$  with respect to the variable  $S$  at  $V = V_{t+1}$ ; namely,

$$\begin{aligned} \partial_S g(V_{t+1}, S) &= R^T (RS - M)(\mathbb{I} - V_{t+1} V_{t+1}^T) \\ &= R^T (RS - RSV_{t+1} V_{t+1}^T - M + MV_{t+1} V_{t+1}^T). \end{aligned} \quad (9)$$

According to [43], the penalty parameter could be set as  $\rho = 1.1 \|R\|^2$ , where  $\|\cdot\|$  is the operator norm of a matrix, i.e., the largest singular value.

The two optimization problems in (8) both have closed-form solutions. More precisely, the  $V$ -subproblem is solved by finding the top  $r$  eigenvectors of a semi-positive definite matrix,  $(M - RS_t)^T (M - RS_t)$ . To do this, one actually just needs to calculate the top  $r$  right singular vectors of  $M - RS_t$ , which is a  $p \times n$  matrix. The solution to the  $S$ -subproblem is given by

$$S_{t+1} = \mathcal{H}_{\lambda/\rho} [S_t - \frac{\partial_S g(V_{t+1}, S)}{\rho}], \quad (10)$$

where  $\mathcal{H}_{\lambda/\rho}[\cdot]$  denotes the entry-wise shrinkage operator with parameter  $\lambda/\rho$ . The whole optimization procedure is also summarized in Algorithm 1.

Empirically, the convergence of Algorithm 1 is determined when the objectives of two adjacent iterations differ by no more than  $10^{-9} \|M\|_F^2$ ; namely,  $|o_{t+1} - o_t| < 10^{-9} \|M\|_F^2$ , where  $o_t$  is the objective computed at the  $t$ th iteration. Under this criterion, the number of iterations for convergence is below 500 in most cases and seldom exceeds 1000. Thus, we consistently set the maximum number of iterations to 1000 in all the experiments.

**Algorithm 2** Compressive Subspace Clustering by RSP

- 
- 1: **input:**  $M$ ,  $R$  and  $k$ .
  - 2: **parameters:**  $r$  and  $\lambda$ .
  - 3: **Output:** clustering results
  - 4: obtain  $\hat{V}_0$  by Algorithm 1, using  $M, R, r$  and  $\lambda$  as the inputs.
  - 5: segment the row vectors of the  $n \times r$  matrix  $\hat{V}_0$  into  $k$  clusters by K-Means.
- 

*C. Clustering Procedure*

Given an estimate (denoted as  $\hat{V}_0$ ) to the authentic row space  $V_0$ , it is rather standard to obtain the final clustering results by using  $|\hat{V}_0 \hat{V}_0^T|$  as an affinity matrix for spectral clustering. This approach often leads to superior clustering results, but it is time consuming especially when  $n$  and  $k$  are both large. For high efficiency, we shall adopt a simple and efficient approach for obtaining the final clustering results based on the estimated row space,  $\hat{V}_0$ , which is just an  $n \times r$  ( $r \ll n$ ) matrix.

Our approach is motivated by the following analyses. When the subspaces are independent and sufficient samples are observed for each subspace, it is known that  $V_0 V_0^T$  is block-diagonal and can lead to correct clustering results [6], [13], [18]. In this case, actually, the  $n \times r_0$  matrix  $V_0$  also owns a structure of block-diagonal. To see why, assume without loss of generality that  $L_0 = [L_1, L_2, \dots, L_k]$ , where  $L_i$  with SVD  $U_i \Sigma_i V_i^T$  is a matrix that stores the samples from the  $i$ th subspace. With these notations, it is easy to see that  $V_0$  is equivalent to a block-diagonal matrix; namely,  $V_0 = \tilde{V}_0 B$  with  $B \in \mathbb{R}^{r_0 \times r_0}$  being an orthogonal matrix (i.e.,  $BB^T = B^T B = \mathbb{I}$ ) and

$$\tilde{V}_0 = \begin{bmatrix} V_1 & 0 & 0 & 0 \\ 0 & V_2 & 0 & 0 \\ 0 & 0 & \ddots & 0 \\ 0 & 0 & 0 & V_k \end{bmatrix}.$$

Given  $\tilde{V}_0$  as above, correct clustering results could be obtained by using directly the K-Means algorithm to segment the rows of  $\tilde{V}_0$  into  $k$  groups. Also, note that the orthogonal matrix  $B$  on the right strictly preserves the inner products among the row vectors. Thus, the clustering results are the same while using  $V_0$  instead of  $\tilde{V}_0$  as inputs to K-Means.

The above analyses illustrate that it is appropriate to get the final clustering results by applying directly K-Means onto the row vectors of  $\tilde{V}_0$ . Algorithm 2 presents the whole procedure of the proposed subspace clustering method. Roughly speaking, this algorithm still falls into the category of spectral-type methods such as SIM, LRR and SSC, which obtain the final subspace clustering results by performing K-Means on a collection of top eigenvectors obtained from the eigenvalue decomposition of some matrix—for example the variants of the self-representation matrices in LRR and SSC. The main difference is that Algorithm 2 discards the construction of  $|\hat{V}_0 \hat{V}_0^T|$  as well as its eigenvalue decomposition so as to produce directly the clustering results based on  $\hat{V}_0$ , achieving high computational efficiency.

*D. Computational Complexity*

After obtaining  $\hat{V}_0$ , it is known that the K-Means clustering step needs  $O(nkr)$  time. So, it remains to make clear the computational complexity of Algorithm 2, in which the computational resources are mostly consumed by its Step 4, i.e., Algorithm 1, which iteratively solves the non-convex optimization problem in (7).

Regarding Algorithm 1, its Step 6—the computation of the matrix  $M - RS$ , needs  $pn + mpn$  elementary operations. The update of the variable  $V$  can be finished by computing the partial- $r$  SVD of a  $p \times n$  matrix and thus has a complexity of  $O(pnr)$ . To compute the gradient given in (9),  $mnp + 4pnr + 4pn$  elementary operations are required. That is, Step 8, which is indeed the most expensive step in Algorithm 1, has an  $O(mnp)$  complexity. The shrinkage operator used in Step 9 is computationally cheap, as it needs only  $O(mn)$  time. In summary, each iteration in Algorithm 1 has an  $O(mnp)$  complexity, thereby the overall complexity of our Algorithm 2 is  $O(mnpl + nkr)$ , where  $l$  is the number of iterations required by Algorithm 1 to get converged.

Up to present, the convergence rate of the alternating proximal method has not been fully understood. Empirically, we have found that at most 1000 iterations are needed for Algorithm 1 to produce near optimal solutions. So, it would be adequate to consider the computational complexity of our RPS as  $O(mnp)$ . Moreover, since the matrix multiplication operators are easily parallelizable, the proposed algorithms are indeed fairly fast, especially when running on Graphics Processing Unit (GPU).

Among the other things, it is worth noting that the iteration number  $l$  would depend on the values of  $\lambda$  and  $r/p$ . In general, larger  $\lambda$  leads to more information loss and, accordingly,  $l$  will be smaller. For example, while  $\lambda$  is sufficiently large (e.g.,  $\lambda = +\infty$ ), the objective in (7) is perfectly minimized by  $\hat{S}_0 = 0$ , and in this case Algorithm 1 converges in only one iteration. Moreover, the iteration number  $l$  also depends on the value of  $r/p$ . In the extreme case of  $r/p \geq 1$ , Algorithm 1 runs only one iteration and outputs the solution of  $\hat{S}_0 = 0$ . Whenever  $\hat{S}_0 = 0$ , our RSP method is almost equivalent to applying directly SIM [13] onto the compressed data matrix  $M$ .

## IV. EXPERIMENTS AND RESULTS

All experiments are conducted on a server equipped with a 64-bit Ubuntu 16.04 operating system, two Intel(R) Xeon(R) E5-2620 v4 2.10GHz CPU processors, 256GB RAM and four NVIDIA Titan X (Pascal) 12GB graphics cards. We have not implemented the algorithms using multiple GPU devices, and thus only one GPU card is randomly chosen by Matlab for accelerating the computations.

*A. Experimental Settings*

1) *Experimental Data:* Notice that the commonly used datasets (e.g., Hopkins155 [44]) have only a few hundreds dimensions, and thus they would not be suitable for being used to verify the merits of compressive robust subspace clustering methods. As a consequence, we create four datasets

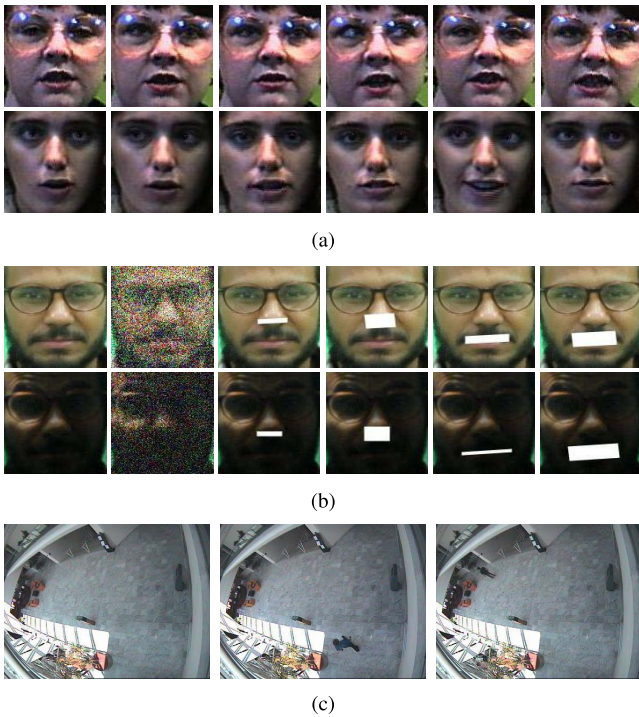


Fig. 1. Examples from the image datasets used in our experiments. The face or digit images in the same row across belong to the same class. (a) EssFace. (b) SoFace. (c) WalVideo.

for experiments, including “SynMat”, “EssFace”, “SoFace” and “WalVideo”.

**1) SynMat:** We first consider randomly generated matrices. A collection of  $200 \times 200$  data matrices are generated according to the model of  $X = L_0 + S_0$ , in which  $L_0$  is created by sampling 100 points from each of 2 randomly generated subspaces, the values in each point are normalized such that the super norm of  $L_0$  is 1, and  $S_0$  is consisting of random Bernoulli  $\pm 1$  values. The dimension of each subspace varies from 1 to 20 with step size 1, and thus the rank of  $L_0$  varies from 2 to 40 with step size 2. The corruption size  $\|S_0\|_0/n$  varies from 0.4 to 8 with step size 0.4. In summary, this dataset contains in total 400 matrices with size  $200 \times 200$ .

**2) EssFace:** The images of the second dataset we used are provided by the University of Essex,<sup>1</sup> so referred to as “EssFace”. This dataset contains in total 7495 images for 375 individuals, each of which has 19 or 20 images. The original images contain background, and no ground truth rectangle is provided. Thus, we utilize the face detector established in [45] to obtain the bounding boxes that contain only the faces. Then we resize the face rectangles into  $100 \times 100$ , resulting in a collection of 7495 10,000-dimensional points for experiments. Figure 1(a) shows some examples selected from this dataset.

**3) SoFace:** The original SoF [46] dataset is a collection of 42,592 face images for 112 individuals, with each individual being involved in multiple photography sessions. The same physical setup is used in each session. In general, this dataset presents several challenges regarding face recognition,

<sup>1</sup>Available at [cswww.essex.ac.uk/mv/allfaces/index.html](http://cswww.essex.ac.uk/mv/allfaces/index.html)

TABLE I  
INFORMATION ABOUT THE FOUR DATASETS USED  
IN THE EXPERIMENTS OF THIS PAPER

name	#class ( $k$ )	#dimension ( $m$ )	#points ( $n$ )	#points in each class
SynMat	2	200	200	100
EssFace	375	10000	7495	19~20
SoFace	2662	10000	26619	8~11
WalVideo	n/a	27648	1379	n/a

e.g., heavy noise, gross occlusion, strong expression, serious blurring and harsh illumination. Since the images for the same individual vary greatly in pose and appearance, it is hard, if not impossible, to form individual-level classes by using the pixel values as inputs for clustering. Thus, instead of identifying the individuals, we aim to group together the images from the same session, i.e., each session is treated as a class. Moreover, we resize the face rectangles into  $100 \times 100$  and discard the images contaminated by blurring or canvas. For the ease of reference, we shall refer to this new version as “SoFace”, which defines a task of segmenting 26,619 data points with dimension 10,000 into 2662 classes. Some example images from this dataset are shown in Figure 1(b).

**4) WalVideo:** In practice, the errors encoded in the sparse component  $S_0$  could correspond to the objects of interest. To show this, we consider a surveillance video selected from the CAVIAR project.<sup>2</sup> The video we considered is a sequence of 1379 frames taken in the entrance lobby of the INRIA Labs, recording the scenes in which one person is walking in straight line, so referred to as “WalVideo” (see Figure 1(c)). This video has a near static background but contains dramatic illuminations. The original frames have a resolution  $384 \times 288$ . We reduce the resolution by half so as to obtain a  $27,648 \times 1379$  data matrix for experiments.

For the ease of reading, we also summarize in Table I the major information of the above four datasets.

**2) Baselines and Evaluation Metrics:** For the sake of comparison, we implement 6 competing methods as follows. Following the suggestions in [31] and [32], we apply three prevalent subspace clustering methods, SIM, LRR and SSC, onto the compressed data matrix  $M \in \mathbb{R}^{p \times n}$ , resulting in three benchmark baselines. Furthermore, we utilize CSMR [37] to recover  $RL_0 \in \mathbb{R}^{p \times n}$  from  $M$  at first, then apply SIM, LRR and SSC onto the recovered matrices (which are estimates to  $RL_0$ ), and in this way we obtain another three competing methods, “CSMR+SIM”, “CSMR+SSC” and “CSMR+LRR”.

Running time and clustering accuracy are used to evaluate the efficiency and effectiveness of subspace clustering methods, respectively. Here, the clustering accuracy is simply the percentage of correctly grouped data points. Also, notice that all the considered methods can be split into two stages: a learning stage that estimates some eigenvector matrix  $V \in \mathbb{R}^{n \times l}$  ( $l = k$  or  $l = r$ ) from data, and a clustering stage that produces the final results by K-Means. So we will report their time consumption separately.

<sup>2</sup>Available at [homepages.inf.ed.ac.uk/rbf/CAVIAR/](http://homepages.inf.ed.ac.uk/rbf/CAVIAR/)

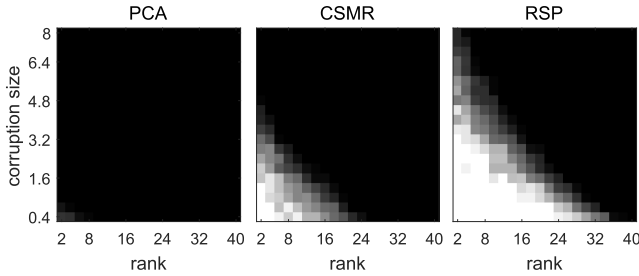


Fig. 2. Results in recovering the randomly generated matrices in SynMat. All the methods are performed on the compressed data matrix  $M$  with  $p = 50$ . The rank  $r_0$  is assumed to be given. The numbers plotted in the above figures are averaged form 20 random trials.

3) *Parameter Configurations:* For the ease of choosing the parameters of various subspace clustering methods, first of all, we normalize the input matrix  $M$  to be column-wisely unit-normed. The parameter  $r$  in SIM plays the same role as in our RSP. So, first we manually tune  $r$  to maximize the accuracy of SIM, then we adjust  $r$  around this estimate for RSP. The parameter  $\lambda$  in RSP is chosen from the range of  $2^{-10} \leq \lambda \leq 2^0$ . Regarding CSMR, which is indeed sensitive to its regularization parameter  $\lambda$ , we try our best to test as more candidates as possible from the range  $2^{-10} \|R\| / \sqrt{\max(p, n)} \leq \lambda \leq 2^{10} \|R\| / \sqrt{\max(p, n)}$ , with the target of maximizing the accuracy of CSMR+SIM. Then the same parameter is used by the other CSMR based methods, e.g., CSMR+LRR. About the key parameter  $\lambda$  in LRR and SSC, we manually select a good estimate from the range of  $0.1 / \sqrt{\log n} \leq \lambda \leq 10 / \sqrt{\log n}$  and  $2^{-10} \leq \lambda \leq 2^{10}$ , respectively.

### B. Results on SynMat

As mentioned in Section III-A, it is possible that RSP strictly succeeds in recovering  $V_0 V_0^T$  under certain conditions. To verify this, we first experiment with the SynMat dataset. The  $200 \times 200$  matrices are projected to  $50 \times 200$  by RP with  $p = 50$ , and task here is to recover the authentic row space by using only the compressed matrix. For each pair of  $r_0$  and  $\|S_0\|_0/n$ , we perform 20 random trials, and thus in this experiment we run 8000 simulations in total. To show the superiorities of RSP, we also consider to recover the target  $V_0 V_0^T$  by PCA and CSMR: PCA estimates  $V_0 V_0^T$  by computing directly the SVD of  $M$ , while CSMR is to firstly obtain an estimate to  $RL_0$  by program (1) and then try obtaining  $V_0 V_0^T$  via performing SVD on the estimate. The accuracy of recovery, i.e., the similarity between  $V_0 V_0^T$  and  $\hat{V}_0 \hat{V}_0^T$ , is measured by Signal-to-Noise Ratio,  $\text{SNR}_{\text{dB}}$ .

The evaluation results are shown in Figure 2, in which each plotted number is a score defined as in the following:

$$\text{score} = \begin{cases} 0, & \text{SNR}_{\text{dB}} < 15, \\ 0.2, & 15 \leq \text{SNR}_{\text{dB}} < 20, \\ 0.5, & 20 \leq \text{SNR}_{\text{dB}} < 30, \\ 1, & \text{SNR}_{\text{dB}} \geq 30. \end{cases} \quad (11)$$

As we can see, PCA works poorly, attaining  $\text{SNR}_{\text{dB}}$  smaller than 15 in almost all the cases. This illustrates that it is

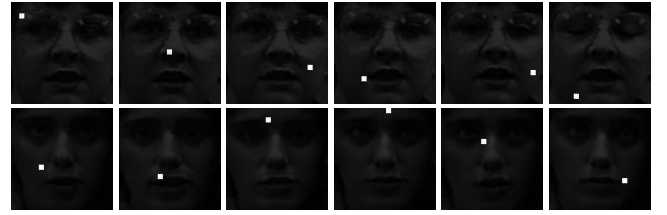


Fig. 3. Examples from the corrupted version of EssFace, with the corruption size being chosen as 25.

TABLE II

EVALUATION RESULTS ON THE CORRUPTED VERSION OF ESSFACE, WITH CORRUPTION SIZE 25 AND  $p = 500$ . OUR GPU IS OF SINGLE PRECISION, THEREBY THE ACCURACY ACHIEVED USING GPU IS SLIGHTLY LOWER THAN USING CPU

method	accuracy (%)	time (seconds)		
		learning	k-means	total
SIM	12.25	<b>24</b>	43	<b>67</b>
CSMR+SIM	12.84	499	42	541
LRR	7.45	105	37	142
CSMR+LRR	7.33	637	37	674
SSC	9.14	1439	44	1483
CSMR+SSC	9.19	2903	45	2948
RSP (CPU)	<b>66.76</b>	1177	<b>20</b>	1197
RSP (GPU)	66.71	257	23	280

unlikely to solve Problem 2 without accessing the sensing matrix  $R$ . Also, it can be seen that CSMR (with  $\lambda = 1.2 \|R\| / \sqrt{\max(p, n)}$ ) succeeds only in limited cases. The reason is that, as aforementioned, CSMR essentially requires  $r_0 \ll \min(p, n)$  such that  $RL_0$  is low rank. Our RSP may partially overcome this limit, thereby RSP (with  $r = r_0$  and  $\lambda = 2^{-7}$ ) can do much better than CSMR in recovering the authentic row space.

### C. Results on EssFace

To get a comprehensive understanding about RSP, we corrupt each image by adding an  $s \times s$  ( $s = 0, 3, 5$ ) spot at a location randomly chosen from the image rectangle. The values in the spot are made to be 5 times as large as the maximum of pixel values so as to suppress the visual information of faces (see Figure 3).

Table II and Figure 4 show the comparison results at  $s = 5$  (i.e., the corruption size is 25) and  $p = 500$ . It can be seen that all of SIM, LRR and SSC produce very poor results. This is because these methods possess no mechanism to disentangle the authentic samples and gross errors. In fact, given only the compressed data  $M$ , there is no way to correctly segment this dataset. The pre-processing of CSMR fails to make any substantial improvement in terms of clustering accuracy. The reason is that  $p = 500$  is not large enough for CSMR to get a good estimate to  $RL_0$ . In contrast, our RSP (with  $r = 40$  and  $\lambda = 2^{-6}$ ) can achieve an accuracy about 67%. This result, in fact, is even slightly better than the best result that SIM, LRR and SSC achieved on the original 10000-dimensional data: Using PCP to pre-process the original data matrix  $X$ , SIM, LRR and SSC attain accuracies of 64.23%, 61.32% and 65.19%, respectively. However, it is

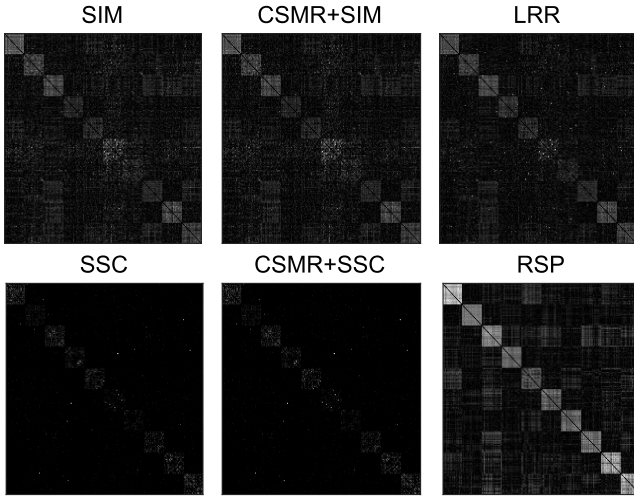


Fig. 4. Visualization of the affinities matrices corresponding to 10 classes in EssFace. For RSP that needs only  $\hat{V}_0$ , we show  $\hat{V}_0\hat{V}_0^T$  for the sake of comparison. Each affinity matrix is post-processed by zeroing-out its diagonal and normalizing its values to have a maximum of 1.

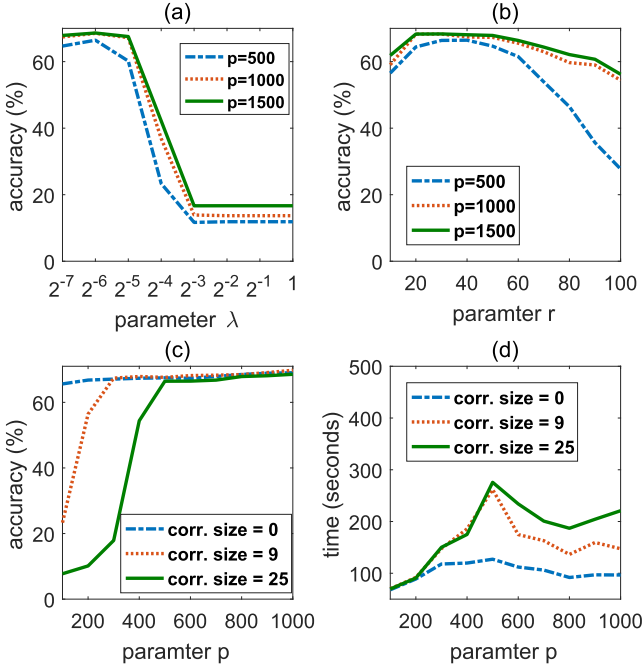


Fig. 5. Explore the performance of RSP under various parametric settings, using EssFace as the experimental data. (a) The parameter  $\lambda$  is varying while  $r = 40$  and corruption size = 25. (b) The parameter  $r$  is varying while  $\lambda = 2^{-6}$  and corruption size = 25. (c-d) The parameter  $p$  is varying while  $\lambda = 2^{-6}$  and  $r = 40$ .

very time-consuming to perform robust subspace clustering on the original high-dimensional data. Namely, PCP spends more than 23 hours in recovering  $L_0$ . In sharp contrast, our RSP (using GPU) needs only about 5 minutes to get good clustering results with accuracy about 67%.

We also investigate the influences of the parameters in RSP as well as the projection number  $p$ . As shown in Figure 5(a), the accuracy of RSP drops dramatically when  $\lambda \geq 2^{-4}$ . This is because, as aforementioned, RSP will converge to the trivial solution  $\hat{S}_0 = 0$  if  $\lambda$  is sufficiently large. Provided that there is no dense noise in the data, theoretically speaking,

TABLE III  
EVALUATION RESULTS ON SoFACE, WITH  $p = 500$

method	accuracy (%)	time (seconds)		
		learning	k-means	total
SIM	52.16	1801	4005	5806
CSMR+SIM	53.82	2809	3998	6807
LRR	48.18	2984	4012	6996
CSMR+LRR	48.01	4247	4025	8272
SSC	53.44	20777	4055	24832
CSMR+SSC	53.79	23070	4087	27157
RSP (CPU)	<b>57.61</b>	1315	<b>310</b>	1625
RSP (GPU)	57.42	<b>214</b>	314	<b>528</b>

there exists  $\lambda^* > 0$  such that RSP works equally well for all  $\lambda \leq \lambda^*$ . However, in practice the white noise is ubiquitous, and thus the performance of RSP slightly degrades while  $\lambda$  is too small. Overall,  $\lambda = 2^{-6}$  is a good choice for this dataset. Regarding the parameter  $r$ , Figure 5(b) shows that RSP could work almost equally well while  $r$  locates in a certain range. This confirms our doctrine that  $r$  is unnecessary to be identical to  $r_0$ . For this dataset,  $r = 40$  is a proper setting, as can be seen from Figure 5(b). As we can see from Figure 5(c), RSP breaks down while  $p$  is too small, and the value of the breaking point depends on the corruption size. More precisely, without the gross corruptions, RSP actually works equally well for a wide range of  $p$ . In the case where the corruption size is 9, RSP breaks down when  $p \leq 200$ . When the corruption size increases to 25, the breaking point becomes  $p \leq 400$ . These phenomena, in general, are consistent with the conditions listed in (6). Figure 5(d) plots the running time as a function of the parameter  $p$ , revealing the phenomenon that the running time of RSP does not increase monotonically with  $p$ . This is because, as discussed earlier, the convergence speed of Algorithm 1 actually depends on  $p$ .

#### D. Results on SoFace

To verify the effectiveness of various methods under the context of compressive robust subspace clustering, we reduce the data dimension to 500 by RP. The comparison results are shown in Table III. In terms of running time, RSP (with  $r = 120$  and  $\lambda = 2^{-5}$ ) distinctly outperforms all the competing methods. In particular, RSP is even much faster than SIM, which is to simply apply SIM onto the compressed matrix  $M \in \mathbb{R}^{500 \times 26619}$ . This is because SoFace has a large number of data points and classes, saying  $n = 26619$  and  $k = 2662$ . In this case, spectral clustering is indeed very time-consuming due to the following two procedures: 1) computing the partial SVD of an  $n \times n$  matrix, and 2) using K-Means to segment a collection of  $n$   $k$ -dimensional points into  $k$  clusters. On this dataset, our Algorithm 1 converges with about 400 iterations, and after that, in sharp contrast, Algorithm 2 only needs to perform K-Means clustering on a set of  $n$   $r$ -dimensional points. Besides of its high computational efficiency, RSP also outperforms the competing methods in the sense of clustering accuracy.

#### E. Results on WalVideo

Unlike the above clustering experiments, in this experiment the input matrix  $M$  is not normalized. This is because we

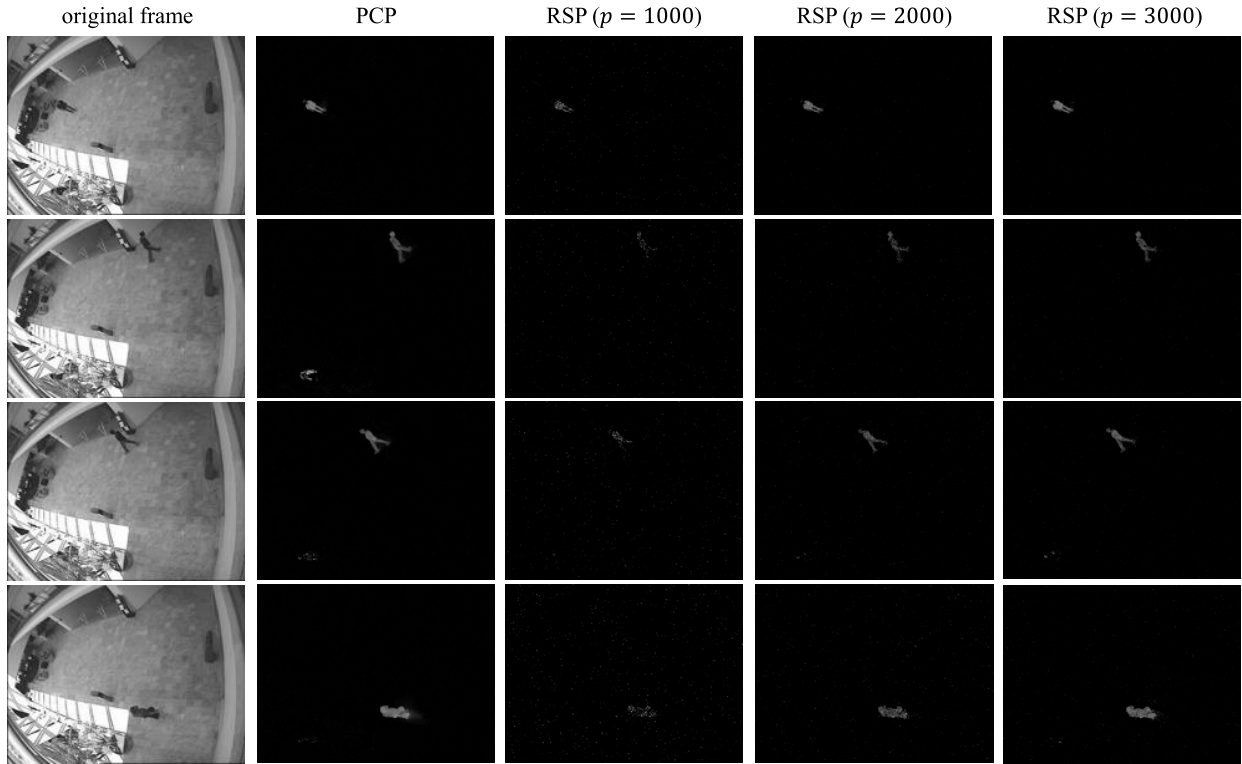


Fig. 6. Moving object detection in surveillance video. Four frames from the WalVideo dataset, with varying illumination. From left to right: the original frame, the sparse component  $|\hat{S}_0|$  obtained by PCP and RSP. The parameters in RSP are set as  $r = 5$  and  $\lambda = 2^{-6}$ .

TABLE IV  
RUNNING TIME ON WALVIDEO. THE PARAMETERS  
OF RSP ARE SET AS  $r = 5$  AND  $\lambda = 2^{-6}$

method	time (seconds)	
	CPU	GPU
PCP	4606	2820
RSP ( $p = 1000$ )	1024	301
RSP ( $p = 2000$ )	1755	469
RSP ( $p = 3000$ )	2299	511

need to visualize the sparse component  $\hat{S}_0$  produced by RSP. Figure 6 shows four frames taken from the WalVideo dataset, which has dramatic illuminations in background. As we can see, RSP with  $p \geq 2000$  works as well as PCP. What is more, in terms of stability against the illumination in background, RSP is even slightly better than PCP. To be more precise, PCP occasionally treats a considerable amount of background illumination as the moving objects (see the second row of Figure 6), while RSP produces more reliable results for the same frame. Since in this dataset the data matrix  $X$  is tall (i.e.,  $m \gg n$ ), the computational complexity of RSP and PCP has the same order. Yet, as shown in Table IV, RSP is still faster than PCP, especially when GPU is used. In particular, our RSP is more parallelizable than PCP, and thus RSP benefits more from GPU than PCP does, as we can see from Table IV.

## V. CONCLUSION

In this paper we studied the problem of *compressive robust subspace clustering*, a significant problem not thoughtfully

explored before. We first mathematically formulated the problem as to recover the row space of the clean data, given only the compressed data  $M$  and sensing matrix  $R$ . Then we devised a simple method termed RSP, which iteratively seeks both the authentic row space and the sparse errors possibly existing in the original high-dimensional data. Extensive experiments with various settings verified the effectiveness and efficiency of RSP.

There are still several problem left for future work. For example, it is better to estimate or learn the hyper-parameter  $r$  from the data. It is also of considerable significant to explore the tensor form and multi-view extensions of the proposed problem.

## ACKNOWLEDGEMENT

Thanks Dr. Yubao Sun and Dr. Meng Wang for sharing with us their opinions.

## REFERENCES

- [1] B. Ella and M. Heikki, "Random projection in dimensionality reduction: Applications to image and text data," in *Proc. 7th ACM SIGKDD Int. Conf. Knowl. Discovery Data Mining*, Aug. 2001, pp. 245–250.
- [2] E. J. Candès, X. Li, Y. Ma, and J. Wright, "Robust principal component analysis?" *J. ACM*, vol. 58, no. 1, pp. 1–37, 2009.
- [3] J. E. Fowler, "Compressive-projection principal component analysis," *IEEE Trans. Image Process.*, vol. 18, no. 10, pp. 2230–2242, Oct. 2009.
- [4] R. Vidal, "Subspace clustering," *IEEE Signal Process. Mag.*, vol. 28, no. 2, pp. 52–68, Mar. 2011.
- [5] G. Liu, Z. Lin, and Y. Yu, "Robust subspace segmentation by low-rank representation," in *Proc. 27th Int. Conf. Mach. Learn.*, 2010, pp. 663–670.

- [6] G. Liu, Z. Lin, S. Yan, J. Sun, Y. Yu, and Y. Ma, "Robust recovery of subspace structures by low-rank representation," *IEEE Trans. Pattern Anal. Mach. Intell.*, vol. 35, no. 1, pp. 171–184, Jan. 2013.
- [7] M. Soltanolkotabi, E. Elhamifar, and E. J. Candès, "Robust subspace clustering," *Ann. Statist.*, vol. 42, no. 2, pp. 669–699, 2014.
- [8] M. Soltanolkotabi and E. J. Candès, "A geometric analysis of subspace clustering with outliers," *Ann. Statist.*, vol. 40, no. 4, pp. 2195–2238, 2012.
- [9] M. A. Fischler and R. Bolles, "Random sample consensus: A paradigm for model fitting with applications to image analysis and automated cartography," *Commun. ACM*, vol. 24, no. 6, pp. 381–395, 1981.
- [10] J. Ho, M.-H. Yang, J. Lim, K.-C. Lee, and D. Kriegman, "Clustering appearances of objects under varying illumination conditions," in *Proc. IEEE Comput. Soc. Conf. Comput. Vis. Pattern Recognit.*, vol. 1, Jun. 2003, pp. 11–18.
- [11] A. Gruber and Y. Weiss, "Multibody factorization with uncertainty and missing data using the EM algorithm," in *Proc. IEEE Comput. Soc. Conf. Comput. Vis. Pattern Recognit.*, vol. 1, Jun./Jul. 2004, pp. 707–714.
- [12] T. Zhang, A. Szelam, and G. Lerman, "Median K-flats for hybrid linear modeling with many outliers," in *Proc. IEEE 12th Int. Conf. Comput. Vis. Workshops (ICCV)*, Sep./Oct. 2009, pp. 234–241.
- [13] J. P. Costeira and T. Kanade, "A multibody factorization method for independently moving objects," *Int. J. Comput. Vis.*, vol. 29, no. 3, pp. 159–179, 1998.
- [14] Y. Ma, A. Yang, H. Derksen, and R. Fossum, "Estimation of subspace arrangements with applications in modeling and segmenting mixed data," *SIAM Rev.*, vol. 50, no. 3, pp. 413–458, 2008.
- [15] Y. Ma, H. Derksen, W. Hong, and J. Wright, "Segmentation of multivariate mixed data via lossy data coding and compression," *IEEE Trans. Pattern Anal. Mach. Intell.*, vol. 29, no. 9, pp. 1546–1562, Sep. 2007.
- [16] E. Elhamifar and R. Vidal, "Sparse subspace clustering," in *Proc. IEEE Conf. Comput. Vis. Pattern Recognit.*, vol. 2, Jun. 2009, pp. 2790–2797.
- [17] G. Chen and G. Lerman, "Spectral curvature clustering (SCC)," *Int. J. Comput. Vis.*, vol. 81, no. 3, pp. 317–330, Mar. 2009.
- [18] Y.-X. Wang, H. Xu, and C. Leng, "Provable subspace clustering: When LRR meets SSC," in *Proc. Adv. Neural Inf. Process. Syst.*, C. J. C. Burges, L. Bottou, M. Welling, Z. Ghahramani, and K. Q. Weinberger, Eds., 2013, pp. 64–72.
- [19] A. Talwalkar, L. Mackey, Y. Mu, S.-F. Chang, and M. I. Jordan, "Distributed low-rank subspace segmentation," in *Proc. IEEE Int. Conf. Comput. Vis.*, Dec. 2013, pp. 3543–3550.
- [20] G. Liu and S. Yan, "Latent low-rank representation for subspace segmentation and feature extraction," in *Proc. Int. Conf. Comput. Vis. (ICCV)*, Nov. 2011, pp. 1615–1622.
- [21] C.-Y. Lu, H. Min, Z.-Q. Zhao, L. Zhu, D.-S. Huang, and S. Yan, "Robust and efficient subspace segmentation via least squares regression," in *Proc. Eur. Conf. Comput. Vis.*, Berlin, Germany: Springer-Verlag, 2012, pp. 347–360.
- [22] P. Favaro, R. Vidal, and A. Ravichandran, "A closed form solution to robust subspace estimation and clustering," in *Proc. IEEE Conf. Comput. Vis. Pattern Recognit. (CVPR)*, Jun. 2011, pp. 1801–1807.
- [23] X. Peng, L. Zhang, and Z. Yi, "Scalable sparse subspace clustering," in *Proc. IEEE Conf. Comput. Vis. Pattern Recognit.*, Jun. 2013, pp. 430–437.
- [24] X. Zhang, F. Sun, G. Liu, and Y. Ma, "Fast low-rank subspace segmentation," *IEEE Trans. Knowl. Data Eng.*, vol. 26, no. 5, pp. 1293–1297, May 2014.
- [25] G. Liu, H. Xu, J. Tang, Q. Liu, and S. Yan, "A deterministic analysis for LRR," *IEEE Trans. Pattern Anal. Mach. Intell.*, vol. 38, no. 3, pp. 417–430, Mar. 2016.
- [26] G. Liu, Q. Liu, and P. Li, "Blessing of dimensionality: Recovering mixture data via dictionary pursuit," *IEEE Trans. Pattern Anal. Mach. Intell.*, vol. 39, no. 1, pp. 47–60, Jan. 2017.
- [27] X. Peng, S. Xiao, J. Feng, W.-Y. Yau, and Z. Yi, "Deep subspace clustering with sparsity prior," in *Proc. 35th Int. Joint Conf. Artif. Intell.*, Jul. 2016, pp. 1925–1931.
- [28] M. Rahmani and G. Atia, "Innovation pursuit: A new approach to the subspace clustering problem," in *Proc. 34th Int. Conf. Mach. Learn.*, vol. 70, 2017, pp. 2874–2882.
- [29] C. Lu, J. Feng, Z. Lin, T. Mei, and S. Yan, "Subspace clustering by block diagonal representation," *IEEE Trans. Pattern Anal. Mach. Intell.*, vol. 41, no. 2, pp. 487–501, Feb. 2018.
- [30] X. Peng, J. Lu, Z. Yi, and R. Yan, "Automatic subspace learning via principal coefficients embedding," *IEEE Trans. Cybern.*, vol. 47, no. 11, pp. 3583–3596, Nov. 2017.
- [31] X. Mao and Y. Gu, "Compressed subspace clustering: A case study," in *Proc. IEEE Global Conf. Signal Inf. Process. (GlobalSIP)*, Dec. 2014, pp. 453–457.
- [32] A. Ruta and F. Porikli, "Compressive clustering of high-dimensional data," in *Proc. 11th Int. Conf. Mach. Learn. Appl.*, vol. 1, Dec. 2012, pp. 380–385.
- [33] E. Elhamifar and R. Vidal, "Sparse subspace clustering: Algorithm, theory, and applications," *IEEE Trans. Pattern Anal. Mach. Intell.*, vol. 35, no. 11, pp. 2765–2781, Nov. 2013.
- [34] E. J. Candès and Y. Plan, "Matrix completion with noise," *Proc. IEEE*, vol. 98, no. 6, pp. 925–936, Jun. 2010.
- [35] G. Liu, Q. Liu, and X. Yuan, "A new theory for matrix completion," in *Proc. Adv. Neural Inf. Process. Syst.*, 2017, pp. 785–794.
- [36] G. Liu, H. Xu, and S. Yan, "Exact subspace segmentation and outlier detection by low-rank representation," *J. Mach. Learn. Res.-Proc. Track*, vol. 22, pp. 703–711, 2012.
- [37] M. Mardani, G. Mateos, and G. B. Giannakis, "Recovery of low-rank plus compressed sparse matrices with application to unveiling traffic anomalies," *IEEE Trans. Inf. Theory*, vol. 59, no. 8, pp. 5186–5205, Aug. 2013.
- [38] J. Wright, A. Ganesh, K. Min, and Y. Ma, "Compressive principal component pursuit," in *Proc. IEEE Int. Symp. Inf. Theory*, Jul. 2012, pp. 1276–1280.
- [39] N. Halko, P. G. Martinsson, and J. A. Tropp, "Finding structure with randomness: Probabilistic algorithms for constructing approximate matrix decompositions," *SIAM Rev.*, vol. 53, no. 2, pp. 217–288, 2011.
- [40] E. J. Candès and T. Tao, "Decoding by linear programming," *IEEE Trans. Inf. Theory*, vol. 51, no. 12, pp. 4203–4215, Dec. 2005.
- [41] Z. Lin, M. Chen, L. Wu, and Y. Ma, "The augmented Lagrange multiplier method for exact recovery of corrupted low-rank matrices," *Dept. Elect. Comput. Eng., UIUC, Champaign, IL, USA, Tech. Rep. UILU-ENG-09-2215*, 2009.
- [42] C. Lu, J. Feng, S. Yan, and Z. Lin, "A unified alternating direction method of multipliers by majorization minimization," *IEEE Trans. Pattern Anal. Mach. Intell.*, vol. 40, no. 3, pp. 527–541, Mar. 2018.
- [43] H. Attouch and J. Bolte, "On the convergence of the proximal algorithm for nonsmooth functions involving analytic features," *Math. Program.*, vol. 116, nos. 1–2, pp. 5–16, Jan. 2009.
- [44] R. Tron and R. Vidal, "A benchmark for the comparison of 3-D motion segmentation algorithms," in *Proc. IEEE Conf. Comput. Vis. Pattern Recognit.*, Jun. 2007, pp. 1–8.
- [45] K. Zhang, Z. Zhang, Z. Li, and Y. Qiao, "Joint face detection and alignment using multitask cascaded convolutional networks," *IEEE Signal Process. Lett.*, vol. 23, no. 10, pp. 1499–1503, Oct. 2016.
- [46] M. Afifi and A. Abdelhamed, "Afif4: Deep gender classification based on adaboost-based fusion of isolated facial features and foggy faces," 2017, arXiv: 1706.04277. [Online]. Available: <https://arxiv.org/abs/1706.04277>



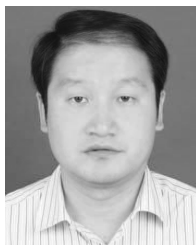
**Guangcan Liu** (M'11–SM'18) received the bachelor's degree in mathematics and the Ph.D. degree in computer science and engineering from Shanghai Jiao Tong University, Shanghai, China, in 2004 and 2010, respectively. He was a Post-Doctoral Researcher with the National University of Singapore, Singapore, from 2011 to 2012, the University of Illinois at Urbana–Champaign, Champaign, IL, USA, from 2012 to 2013, Cornell University, Ithaca, NY, USA, from 2013 to 2014, and Rutgers University, Piscataway, NJ, USA, in 2014.

Since 2014, he has been a Professor with the School of Automation, Nanjing University of Information Science and Technology, Nanjing, China. His research interests touch on the areas of pattern recognition, computer vision, and signal processing.



**Zhao Zhang** (SM'17) received the Ph.D. degree from the Department of Electronic Engineering (EE), City University of Hong Kong, in 2013. He has been a Visiting Research Engineer with the National University of Singapore since 2012. He has also been visiting the National Laboratory of Pattern Recognition (NLPR), Chinese Academy of Sciences (CAS), since 2012. He is currently an Associate Professor with the School of Computer Science and Technology, Soochow University, Suzhou, China. His current research interests include data mining

and statistical machine learning, pattern recognition, and image analysis.



**Qingshan Liu** (M'05–SM'08) received the Ph.D. degree from the National Laboratory of Pattern Recognition, Chinese Academy of Sciences, Beijing, China, in 2003, and the M.S. degree from Southeast University, Nanjing, China, in 2000. He was an Associate Professor with the National Laboratory of Pattern Recognition. He was an Assistant Research Professor with the Department of Computer Science, Computational Biomedicine Imaging and Modeling Center, Rutgers University, The State University of New Jersey, Piscataway, NJ, USA, from 2010 to

2011. He is currently a Professor with the School of Information and Control Engineering, Nanjing University of Information Science and Technology, Nanjing, China. His research interests include image and vision analysis, including face image analysis, graph- and hypergraph-based image and video understanding, medical image analysis, and event-based video analysis. He was a recipient of the President Scholarship of the Chinese Academy of Sciences in 2003.



**Hongkai Xiong** (M'01–SM'10) received the Ph.D. degree from Shanghai Jiao Tong University (SJTU), Shanghai, China, in 2003. He was an Associate Professor from 2005 to 2011 and an Assistant Professor from 2003 to 2005. From 2007 to 2008, he was a Research Scholar with the Department of Electrical and Computer Engineering, Carnegie Mellon University (CMU), Pittsburgh, PA, USA. From 2011 to 2012, he was a Scientist with the Division of Biomedical Informatics, University of California at San Diego (UCSD), San Diego, CA,

USA. Since 2003, he has been with the Department of Electronic Engineering, SJTU, and has also been with UCSD, San Diego, CA, USA. He is currently a Distinguished Professor with the Department of Electronic Engineering, Shanghai Jiao Tong University (SJTU).

He has coauthored a Best Paper in IEEE BMSB 2013, a Best Student Paper in VCIP 2014, a Top 10% Paper Award in VCIP 2016, and a Top 10% Paper Award in MMSP 2011. His research interests include multimedia signal processing, image and video coding, multimedia communication and networking, computer vision, biomedical informatics, machine learning. He published more than 200 refereed journal and conference papers.

Dr. Xiong's research projects are funded by NSF, QUALCOMM, Microsoft, and Intel. He received the 2009 New Century Excellent Talent Award from Ministry of Education of China, the 2010 and 2013 SJTU SMC-A Excellent Young Faculty Awards, the 2013 Shanghai Shu Guang Scholar Award, the 2014 Shanghai Youth Science and Technology Talent Award, the 2014 National Science Fund for Distinguished Young Scholar Award from Natural Science Foundation of China (NSFC), the 2016 Yangtze River Scholar Distinguished Professor Award from Ministry of Education, China, the 2017 Shanghai Academic Research Leader Talent Award, the 2017 Baosteel Excellent Faculty Award, and the 2017 Science and Technology Innovative Leader Talent Award in Ten Thousand Talents Program. He has been granted 2011 and 2017 First Prizes of the Shanghai Technology Innovation Award for research achievements on Network-oriented Video Processing and Dissemination. He is an Associate Editor of the IEEE TRANSACTIONS ON CIRCUITS AND SYSTEMS FOR VIDEO TECHNOLOGY (TCSVT).